Accelerating Kohn–Sham Response Theory using Density-fitting and the Auxiliary-Density-Matrix Method

Chandan Kumar,[1, a)] Heike Fliegl,[1] Frank Jensen,[2] Andrew M. Teale,[3, 1] Simen Reine,[1, b)] and Thomas Kjærgaard[4, c)]

[1)] *Centre for Theoretical and Computational Chemistry, Department of Chemistry, University of Oslo, P.O.Box 1033, N-1315 Blindern, Norway*

[2)] *Department of Chemistry, Aarhus University, Langelandsgade 140, DK-8000 Aarhus C, Denmark*

[3)] *Department of Physical and Theoretical Chemistry, University of Nottingham, University Park, Nottingham NG7 2RD, United Kingdom*

[4)] *qLEAP Center for Theoretical Chemistry, Department of Chemistry, Aarhus University, Langelandsgade 140, DK-8000 Aarhus C, Denmark*

An extension of the formulation of time dependent density functional response theory (TDDFT) that includes approximate Fock/Kohn-Sham matrices is presented. The new framework allows for flexible use of approximate methods to calculate the Coulomb and exchange integrals such as the resolution of the identity (RI) and the auxiliary-density matrix method (ADMM) in an efficient manner. Other alternative approximate approaches for the Coulomb and exchange integrals can easily be accessed allowing for systematic performance tests of different methods. The new approximate Kohn-Sham response theory framework has been implemented in the program LSDalton. It has been tested for both linear and quadratic response properties: vertical excitation energies, polarizabilities and hyperpolarizabilities. The results indicate that density fitting of the Coulomb contribution can be used without hesitation for all properties studied here. The impact of the additional approximations in the ADMM treatment of exchange have been carefully assessed and it is shown that the method yields high accuracy for ground-state and excitation energies, whereas for polarizabilities and hyperpolarizabilities the accuracy to performance ratio is less satisfactory.

I. INTRODUCTION

In molecular electronic-structure theory, an essential step is the evaluation of two-electron integrals over one-electron basis functions. The explicit evaluation of these integrals comes at a high computational cost, and from the dawn of quantum chemistry, approximations have been introduced both to speed up molecular calculations and to reduce memory requirements. Such approximate methods have been widely developed for the calculation of energies and gradients, but less attention is given to developing these methods for the calculation of molecular properties.

The most widely used approach to approximate the Coulomb and exchange integrals is density fitting[1–21], also known as the resolution-of-the-identity (RI) approximation. In this approximation products of two one-electron basis functions are expanded in one-center auxiliary orbitals, and thus, the evaluation of four-center two-electron integrals is replaced by the evaluation of two- and three-center two-electron integrals and the solution of a set of linear equations. RI significantly improves performance with a limited impact on the accuracy and has therefore been applied to Hartree-Fock(HF)/Kohn-Sham(KS) theory, as well as correlated methods[21–26]. An important alternative approach is the Cholesky-

decomposition (CD) technique[27–31] which to a large extent can be thought of as a special kind of density fitting where the basis of auxiliary functions are obtained from the set of products between two one-electron basis functions through Cholesky-decomposition.

Combined with *J*-engine techniques[32–34] RI gives tremendous speed-ups[7,8] for Coulomb-like contributions. Although still applicable to exchange[9–12,15,16,19,20], the RI methodology does not exhibit the same favourable performance gains as for the Coulomb integrals. Alternative schemes such as the auxiliary-density-matrix method (ADMM)[35,36] and the chain-of-spheres algorithm (COSX)[37] have therefore been developed specifically for the exchange contribution. In ADMM, the exchange energy is split into two parts. One part consists of the exact HF exchange evaluated in a small auxiliary atomic basis set (from an auxiliary density matrix); the second part is a first-order correction term, evaluated as the difference between the generalized gradient approximation (GGA) exchange in the full and auxiliary basis sets. The auxiliary density matrix can be obtained by means of projection from the full density matrix fulfilling various constraints, as discussed by Guidon *et al.*[35] and Merlot *et al.*[36]. The COSX approximation builds on the use of semi-numerical integration techniques, first introduced by Friesner in the pseudo-spectral method[38–40] and later refined in the COSX approach by Neese *et al.*[37]. In this approach the Coulomb potentials of products of two one-electron basis functions are evaluated analytically on a grid, followed by a numerical integration over the second electron. Reported speed-ups are of up to two orders of magnitude relative to calculations involving explicit

exchange-matrix formation[37]. In this work we explore how these techniques may be exploited further in the calculation of molecular properties using response theory.

In response function theory[41–49] we determine the time development of an observable when the molecular system is subjected to an external electric or magnetic field. The frequency dependent perturbation causes the wave function to become frequency dependent. The response of the observable may be expanded in powers of the field strength: the linear response of the system is determined by the linear response function, the quadratic response by the quadratic response function, and so on[50].

The linear response function therefore represents the first-order correction to the expectation value of choice. The quadratic-response function represents the second order correction to the expectation value of choice and so on. For example, the frequency-dependent polarizability and hyper-polarizability may be evaluated from the linear and quadratic response functions, respectively. In the present work we investigate static (frequency independent) polarizabilities and hyperpolarizabilities. From the poles and residues of the response functions, additional molecular properties can be obtained, including vertical excitation energies to electronically excited states, strength parameters for (multi-photon) transitions to these states, and excited-state properties[41].

Recently, Ringholm et al.[51] presented an approach involving recursion for the open-ended calculation of response properties based on the density matrix-based quasi-energy formulation of the Kohn–Sham density functional response theory using perturbation- and time-dependent basis sets of Thorvaldsen et al.[44]. This approach was extended by Friese et al. to enable the calculation of single residues of response functions[52,53]. Very recently, this approach has furthermore been extended to include molecular environment effects by the polarizable embedding model[54].

The RI approximation has been extensively used in connection with CC2 molecular properties[55–64], but has also been used in connection with the coupled perturbed Kohn–Sham equations[65]. It has also been used in TD-DFT in connection with excitation energies, excited state gradients and frequency-dependent optical rotation calculations[66–70]. Recently, Kumar et. al. showed that density fitting can also be applied for the efficient calculation of nuclear magnetic resonance shielding tensors[71]. Ref. 66 and 69 concluded that the auxiliary basis sets developed for ground state calculations are sufficient for most TDDFT applications, although in some cases additional diffuse basis functions must be included. Ref. 69 reported that the total computational effort for excited state optimizations is reduced by at least a factor of 4-6 by the RI-J approximation, with corresponding RI-J errors of 0.01-0.02 eV. The RI-J errors in optimized bond lengths and angles amounted to less then 0.5 pm and 1 degree, respectively. These deviations are usually much smaller than errors due to the incompleteness of the one-particle basis set.

In the present paper we present a method for the computation of response functions within the self-consistent-field (SCF) theories HF and KS density functional theory (DFT) and the extension to include ADMM, density fitting and other approximations in the construction of the Fock/Kohn-Sham matrix. The new formulation of approximate response theory presented in this work is very general and works in principle for all approximations where the approximate Kohn-Sham matrix can be defined as the density matrix derivative of the approximate energy. It allows to easily accommodate future approximate methods that may differ from ADMM or RI in HF/KS response theory. The formulation makes it clear that density fitting/RI can be straight forwardly applied in the context of response theory, and the limited number of benchmark studies is therefore surprising.

The approximate response theory formulation introduced in this work is asymptotic linear scaling assuming that sparse matrix algebra is used. However, the focus of the present study is not on the scaling of the approach with system size. Instead we use the new methodology to investigate the impact of several different approximations such as RI and ADMM on the accuracy of linear, quadratic and cubic response properties. As examples we consider vertical excitation energies, static polarizabilities and static hyperpolarizabilities. We commence in Section II by introducing the theoretical framework for the response calculations. In Section III A we show how this framework can easily accommodate a range of techniques for approximating the most costly contribution arising from the Coulomb and exchange integrals. In Section V we present results for a range of molecular response properties to gauge the relative accuracy of these techniques in practical application. Finally in Section VI we make some concluding remarks and discuss directions for future work.

II. THEORY

In order to provide a framework to easily introduce ADMM and other approximate methods in HF/KS response theory we first derive response theory in a formulation where the Fock/Kohn-Sham matrix takes a center stage. The derivation follows the response theory method of Larsen et al.[47] with a few modifications emphasizing the role of the Fock/Kohn-Sham matrix, followed by an adaptation to ADMM and RI theories. The derivation assumes that all basis sets employed do not depend on the perturbation. Hence no London[72](gauge including) atomic orbitals nor geometric perturbations are considered in the present work.

A. Time evolution of the Kohn–Sham system

In Kohn-Sham (KS) density-functional theory (DFT), the time evolution of the spin orbitals, in presence of a

time dependent perturbation $V(\mathbf{r}_1, t)$, is governed by the time-dependent Schrödinger equation[73–76],

$$[f_{\mathrm{KS}}(\mathbf{r}_1, t) + V(\mathbf{r}_1, t)]\phi_j(\mathbf{r}_1, t) = i\frac{d\phi_j(\mathbf{r}_1, t)}{dt}, \quad (1)$$

where we have introduced the Kohn-Sham operator $f_{\mathrm{KS}}(\mathbf{r}_1, t) = h(\mathbf{r}_1) + j(\mathbf{r}_1, t) + v_{\mathrm{xc}}(\mathbf{r}_1, t)$, which we choose to define without the perturbation $V(\mathbf{r}_1, t)$. The constituents of the Kohn-Sham operator are given through their matrix definitions in detail later in Eq. (6). The Kohn-Sham potential f_{KS} is defined as the functional derivative of the unperturbed energy functional

$$f_{\mathrm{KS}}(\mathbf{r}_1, t) = \left.\frac{\delta E[\rho]}{\delta\rho(\mathbf{r}_1)}\right|_{\rho(\mathbf{r}_1)=\rho(\mathbf{r}_1, t)} \quad (2)$$

which depends on the perturbation $V(\mathbf{r}_1, t)$ through the density

$$\rho(\mathbf{r}, t) = \sum_{\mu\nu} \chi_\mu^*(\mathbf{r})\chi_\nu(\mathbf{r})D_{\nu\mu}, \quad (3)$$

where $\mathbf{D}$ is the time dependent density matrix in the atomic-orbital (AO) basis and $\chi(\mathbf{r})$ denotes the AO basis functions. In the case of hybrid functionals f_{KS} may be supplemented by an orbital dependent term of the form, $w \cdot k(\mathbf{r}_1, \mathbf{r}_2, t)$, where w is the weight of orbital dependent exchange and $k(\mathbf{r}_1, \mathbf{r}_2, t)$ is the derivative of the exchange energy with respect to the orbitals, as is used in Hartree–Fock theory.

Eq. (1) may be rewritten as a matrix equation using the expansion in AOs χ_μ

$$\phi_i(\mathbf{r}_1, t) = \sum_\mu C_{\mu i}\chi_\mu(\mathbf{r}_1), \quad (4)$$

to obtain[47]

$$\left(\mathbf{F}(\mathbf{D}) + \mathbf{V} - i\mathbf{S}\frac{\partial}{\partial t}\right)\mathbf{C} = \mathbf{S}\mathbf{C}\lambda \quad (5)$$

with

$$F_{\mu\nu}(\mathbf{D}) = \frac{\delta E}{\delta D_{\mu\nu}} = h_{\mu\nu} + J_{\mu\nu} + wK_{\mu\nu} + K_{\mu\nu}^{\mathrm{xc}}$$

$$h_{\mu\nu} = \int \chi_\mu(\mathbf{r})\left(-\frac{1}{2}\nabla_1^2 + \sum_I \frac{Z_I}{|\mathbf{r} - \mathbf{R}_I|}\right)\chi_\nu(\mathbf{r})d\mathbf{r}$$

$$J_{\mu\nu}(\mathbf{D}) = \sum_{\rho\sigma} (\mu\nu|\rho\sigma)D_{\rho\sigma}$$

$$K_{\mu\nu}(\mathbf{D}) = \sum_{\rho\sigma} (\mu\sigma|\rho\nu)D_{\rho\sigma}$$

$$F_{\mu\nu}^{\mathrm{xc}}(\rho) = \int \chi_\mu(\mathbf{r})v_{\mathrm{xc}}(\mathbf{r}, t)\chi_\nu(\mathbf{r})d\mathbf{r}$$

$$V_{\mu\nu} = \int \chi_\mu(\mathbf{r})V(\mathbf{r}, t)\chi_\nu(\mathbf{r})d\mathbf{r}$$

$$S_{\mu\nu} = \int \chi_\mu(\mathbf{r})\chi_\nu(\mathbf{r})d\mathbf{r}$$

$$(\mu\nu|\rho\sigma) = \iint \chi_\mu(\mathbf{r}_1)\chi_\nu(\mathbf{r}_1, t)\frac{1}{r_{12}}\chi_\rho(\mathbf{r}_2)\chi_\sigma(\mathbf{r}_2)d\mathbf{r}_1 d\mathbf{r}_2. \quad (6)$$

Eq. (5) reduces to the SCF equation in the perturbation free limit ($\mathbf{V} = 0$) and therefore time-independent limit

$$\mathbf{F}(\mathbf{D})\mathbf{C} = \mathbf{S}\mathbf{C}\lambda. \quad (7)$$

Multiplying Eq. (5) with $\mathbf{C}^T\mathbf{S}$ from the right, subtracting the complex conjugate equation and introducing the density matrix in the AO basis $\mathbf{D} = \mathbf{C}\mathbf{C}^T$ we may write this equation as[47]

$$(\mathbf{F}(\mathbf{D}) + \mathbf{V})\mathbf{D}\mathbf{S} - \mathbf{S}\mathbf{D}(\mathbf{F}(\mathbf{D}) + \mathbf{V}) = i\mathbf{S}\dot{\mathbf{D}}\mathbf{S} \quad (8)$$

We use the short hand notation $\dot{D} = \frac{\partial D}{\partial t}$ for the time derivative of the density matrix. Eq. (8) reduces to the standard stationary SCF condition $\mathbf{F}\mathbf{D}_0\mathbf{S} - \mathbf{S}\mathbf{D}_0\mathbf{F} = \mathbf{0}$ in the perturbation free limit, with $\mathbf{D}_0$ being the optimized AO density matrix for the unperturbed system.

B. Kohn Sham matrix expansion

We use an exponential parametrization of the density matrix

$$\mathbf{D}(\mathbf{X}(t)) = \exp(-\mathbf{X}(t)\mathbf{S})\mathbf{D}\exp(\mathbf{S}\mathbf{X}(t)) \quad (9)$$

where $\mathbf{X}(t)$ is an anti-hermitian matrix. Furthermore it is assumed that the symmetry, trace and idempotency conditions are imposed[77,78], which implies that the reference density matrix $\mathbf{D}$ also fulfills these conditions. The transformed density matrix $\mathbf{D}(\mathbf{X})$, may then be evaluated using the the asymmetric Baker-Campbell-Hausdorff (BCH) expansion

$$\mathbf{D}(\mathbf{X}) = \mathbf{D}_0 + [\mathbf{D}, \mathbf{X}]_{\mathbf{S}} + \frac{1}{2}[[\mathbf{D}, \mathbf{X}], \mathbf{X}] + \cdots \quad (10)$$

where we have defined the S-commutator:

$$[\mathbf{D}, \mathbf{X}]_{\mathbf{S}} = \mathbf{D}\mathbf{S}\mathbf{X} - \mathbf{X}\mathbf{S}\mathbf{D}. \tag{11}$$

When performing a Taylor expansion of the Kohn-Sham matrix $\mathbf{F}$ around the optimized AO density matrix for the unperturbed state one obtains the following expression

$$\mathbf{F}(\mathbf{D}(\mathbf{X})) = \mathbf{F}(\mathbf{D}_0) + \left.\frac{\partial \mathbf{F}}{\partial \mathbf{D}(\mathbf{X})}\right|_{\mathbf{D}(\mathbf{X})=\mathbf{D}_0} (\mathbf{D}(\mathbf{X}) - \mathbf{D}_0)$$
$$+ \frac{1}{2} \left.\frac{\partial^2 \mathbf{F}}{\partial \mathbf{D}(\mathbf{X})^2}\right|_{\mathbf{D}(\mathbf{X})=\mathbf{D}_0} (\mathbf{D}(\mathbf{X}) - \mathbf{D}_0)^2 + \cdots \tag{12}$$

Since we are typically interested in derivatives contracted with a matrix $\mathbf{M}$, thus

$$\left.\frac{\partial \mathbf{J}(\mathbf{D}(\mathbf{X}))}{\partial \mathbf{D}(\mathbf{X})}\right|_{\mathbf{D}(\mathbf{X})=\mathbf{D}_0} \mathbf{M} = \mathbf{J}(\mathbf{M})$$
$$\left.\frac{\partial \mathbf{K}(\mathbf{D}(\mathbf{X}))}{\partial \mathbf{D}(\mathbf{X})}\right|_{\mathbf{D}(\mathbf{X})=\mathbf{D}_0} \mathbf{M} = \mathbf{K}(\mathbf{M}) \tag{13}$$
$$\left.\frac{\partial \mathbf{F}^{\text{xc}}(\mathbf{D}(\mathbf{X}))}{\partial \mathbf{D}(\mathbf{X})}\right|_{\mathbf{D}(\mathbf{X})=\mathbf{D}_0} \mathbf{M} = \mathbf{K}^{\text{xc}}(\mathbf{M})$$

where

$$\mathbf{K}^{\text{xc}}(\mathbf{M}) = \iint \chi_\mu(\mathbf{r}) \sum_{\rho\sigma} \frac{\delta v_{\text{xc}}}{\delta\rho(\mathbf{r}, t)} \chi_\rho(\mathbf{r}) \chi_\sigma(\mathbf{r}) \mathbf{M}_{\rho\sigma} \chi_\nu(\mathbf{r}) d\mathbf{r} d\mathbf{r}' \tag{14}$$

Denoting the first derivative of the KS matrix contracted with a general matrix $\mathbf{M}$ as $\mathbf{G}(\mathbf{M})$, we then have

$$\mathbf{G}(\mathbf{M}) = \left.\frac{\partial \mathbf{F}}{\partial \mathbf{D}(\mathbf{X})}\right|_{\mathbf{D}(\mathbf{X})=\mathbf{D}_0} \mathbf{M}$$
$$= \mathbf{J}(\mathbf{M}) + w \cdot \mathbf{K}(\mathbf{M}) + \mathbf{K}^{\text{xc}}(\mathbf{M}). \tag{15}$$

For the second and higher order Kohn-Sham matrix derivatives only exchange-correlation contributions remain, and we define

$$T(\mathbf{N}, \mathbf{M}) = \left.\frac{\partial^2 \mathbf{F}(\mathbf{D}(\mathbf{X}))}{\partial \mathbf{D}(\mathbf{X})^2}\right|_{\mathbf{D}(\mathbf{X})=\mathbf{D}_0} (\mathbf{N}, \mathbf{M}) = T^{\text{xc}}(\mathbf{N}, \mathbf{M})$$

$$T^{\text{xc}}_{\phi\xi}(\mathbf{N}, \mathbf{M}) = \sum_{\rho\sigma\eta\epsilon} M_{\rho\sigma} N_{\eta\epsilon} \iiint \chi_\phi^*(\mathbf{r}) \chi_\xi(\mathbf{r}) \chi_\rho^*(\mathbf{r}') \tag{16}$$
$$\chi_\sigma(\mathbf{r}') \chi_\eta^*(\mathbf{r}'') \chi_\epsilon(\mathbf{r}'') \frac{\delta^2 v_{\text{xc}}(\mathbf{r})}{\delta\rho(\mathbf{r})^2} d\mathbf{r} d\mathbf{r}' d\mathbf{r}''$$

to obtain:

$$\mathbf{F}(\mathbf{D}(\mathbf{X})) = \mathbf{F}(\mathbf{D}_0) + \mathbf{G}(\mathbf{D}(\mathbf{X}) - \mathbf{D}_0)$$
$$+ \frac{1}{2}\mathbf{T}(\mathbf{D}(\mathbf{X}) - \mathbf{D}_0, \mathbf{D}(\mathbf{X}) - \mathbf{D}_0) + \cdots \tag{17}$$

The parameters $\mathbf{X}$ must then be determined in the presence of the perturbation.

C. Response Equation

The set of parameters $\mathbf{X}(t)$ can be expanded in orders of the perturbation

$$\mathbf{X}(t) = \mathbf{X}^{(1)}(t) + \mathbf{X}^{(2)}(t) + \cdots \tag{18}$$

where the zero-order coefficients vanish since the reference state is optimized. Using Eq. (10) and Eq. (17) we may expand Eq. (8) in orders of the perturbation. The parameters $\mathbf{X}^{(n)}(t)$ can now be determined by requiring Eq. (8) to be valid to each order of the perturbation. The resulting equation containing the first order contributions $\mathbf{X}^{(1)}(t)$ is called the *linear response equation*, similarly the second order $\mathbf{X}^{(2)}(t)$ parameters are obtained from the *quadratic response equation* and so forth.

1. Linear Response Equation

The terms that contribute to the evaluation of the $\mathbf{X}^{(1)}(t)$ are

$$\mathbf{G}([\mathbf{D}, \mathbf{X}^{(1)}]_{\mathbf{S}})\mathbf{D}\mathbf{S} - \mathbf{S}\mathbf{D}\mathbf{G}([\mathbf{D}, \mathbf{X}^{(1)}]_{\mathbf{S}})$$
$$+ \mathbf{F}(\mathbf{D})[\mathbf{D}, \mathbf{X}^{(1)}]_{\mathbf{S}}\mathbf{S} - \mathbf{S}[\mathbf{D}, \mathbf{X}^{(1)}]_{\mathbf{S}}\mathbf{F}(\mathbf{D}) \tag{19}$$
$$+ \mathbf{V}\mathbf{D}\mathbf{S} - \mathbf{S}\mathbf{D}\mathbf{V} = i\mathbf{S}[\mathbf{D}, \dot{\mathbf{X}}]_{\mathbf{S}}\mathbf{S}$$

To solve this first-order equation we use the Fourier expansion of $X^{(1)}(t)$

$$X^{(1)}(t) = \int_{-\infty}^{\infty} \exp(-i\omega t) X^{(1)}(\omega) d\omega \tag{20}$$

and obtain:

$$\mathbf{G}([\mathbf{D}, \mathbf{X}^{(1)}(\omega)]_{\mathbf{S}})\mathbf{D}\mathbf{S} - \mathbf{S}\mathbf{D}\mathbf{G}([\mathbf{D}, \mathbf{X}^{(1)}(\omega)]_{\mathbf{S}})$$
$$+ \mathbf{F}(\mathbf{D})[\mathbf{D}, \mathbf{X}^{(1)}(\omega)]_{\mathbf{S}}\mathbf{S} - \mathbf{S}[\mathbf{D}, \mathbf{X}^{(1)}(\omega)]_{\mathbf{S}}\mathbf{F}(\mathbf{D}) \tag{21}$$
$$+ \mathbf{V}\mathbf{D}\mathbf{S} - \mathbf{S}\mathbf{D}\mathbf{V} = -\omega\mathbf{S}[\mathbf{D}, \mathbf{X}(\omega)]_{\mathbf{S}}\mathbf{S}.$$

It can also be written as[48,79]

$$\left(\mathbf{E}^{[2]} - \omega\mathbf{S}^{[2]}\right) \mathbf{X}(\omega) = \mathbf{V}\mathbf{D}\mathbf{S} - \mathbf{S}\mathbf{D}\mathbf{V} \tag{22}$$

with the generalized Hessian $\mathbf{E}^{[2]}$ defined through the transformation

$$\mathbf{E}^{[2]}\mathbf{X}(\omega) = -\mathbf{G}([\mathbf{D}, \mathbf{X}^{(1)}(\omega)]_{\mathbf{S}})\mathbf{D}\mathbf{S} + \mathbf{S}\mathbf{D}\mathbf{G}([\mathbf{D}, \mathbf{X}^{(1)}(\omega)]_{\mathbf{S}})$$
$$- \mathbf{F}[\mathbf{D}, \mathbf{X}^{(1)}(\omega)]_{\mathbf{S}}\mathbf{S} + \mathbf{S}[\mathbf{D}, \mathbf{X}^{(1)}(\omega)]_{\mathbf{S}}\mathbf{F}, \tag{23}$$

and the generalized metric matrix $\mathbf{S}^{[2]}$ through

$$\mathbf{S}^{[2]}\mathbf{X}(\omega) = \mathbf{S}[\mathbf{D}, \mathbf{X}(\omega)]_{\mathbf{S}}\mathbf{S}. \tag{24}$$

The excitation energies are identified as the poles of the linear response equation and are therefore solutions to the generalized eigenvalue problem defined below.

$$\mathbf{E}^{[2]}\mathbf{X}_f = \mathbf{S}^{[2]}\mathbf{X}_f \omega_f \tag{25}$$

2.   Quadratic Response Equation

The terms that contribute to the evaluation of the $\mathbf{X}^{(2)}(t)$ are

$$
\begin{aligned}
&-\Bigg(\mathbf{G}([\mathbf{D}, \mathbf{X}^{(2)}(\omega_1, \omega_2)]_\mathbf{S}) \\
&+ P_{12}\mathbf{G}(\frac{1}{2}[[\mathbf{D}, \mathbf{X}^{(1)}(\omega_1)], \mathbf{X}^{(2)}(\omega_2)]) \\
&+ \frac{1}{2}P_{12}\mathbf{T}([\mathbf{D}, \mathbf{X}^{(1)}(\omega_1)]_\mathbf{S}, [\mathbf{D}, \mathbf{X}^{(1)}(\omega_2)]_\mathbf{S})\Bigg)\mathbf{DS} \\
&+ \mathbf{SD}\Bigg(\mathbf{G}([\mathbf{D}, \mathbf{X}^{(2)}(\omega_1, \omega_2)]_\mathbf{S}) \\
&+ P_{12}\mathbf{G}(\frac{1}{2}[[\mathbf{D}, \mathbf{X}^{(1)}(\omega_1)], \mathbf{X}^{(2)}(\omega_2)]) \\
&+ \frac{1}{2}P_{12}\mathbf{T}([\mathbf{D}, \mathbf{X}^{(1)}(\omega_1)]_\mathbf{S}, [\mathbf{D}, \mathbf{X}^{(1)}(\omega_2)]_\mathbf{S})\Bigg) \\
&- P_{12}\mathbf{G}([\mathbf{D}, \mathbf{X}^{(1)}(\omega_1)]_\mathbf{S})[\mathbf{D}, \mathbf{X}^{(1)}(\omega_2)]_\mathbf{S}\mathbf{S} \\
&- \frac{1}{2}P_{12}\mathbf{F}(\mathbf{D}_0)[[\mathbf{D}, \mathbf{X}^{(1)}(\omega_1)], \mathbf{X}^{(1)}(\omega_2)]\mathbf{S} \\
&+ P_{12}\mathbf{S}[\mathbf{D}, \mathbf{X}^{(1)}(\omega_1)]_\mathbf{S}\mathbf{G}([\mathbf{D}, \mathbf{X}^{(1)}(\omega_2)]_\mathbf{S}) \\
&+ \frac{1}{2}P_{12}\mathbf{S}[[\mathbf{D}, \mathbf{X}^{(1)}(\omega_1)], \mathbf{X}^{(1)}(\omega_2)]\mathbf{F}(\mathbf{D}_0) \\
&- \mathbf{F}[\mathbf{D}, \mathbf{X}^{(2)}(\omega_1, \omega_2)]_\mathbf{S}\mathbf{S} + \mathbf{S}[\mathbf{D}, \mathbf{X}^{(2)}(\omega_1, \omega_2)]_\mathbf{S}\mathbf{F} \\
&- (\omega_1 + \omega_2)\mathbf{S}[\mathbf{D}, \mathbf{X}^{(2)}(\omega_1, \omega_2)]_\mathbf{S}\mathbf{S} \\
&- \frac{1}{2}(\omega_1 + \omega_2)P_{12}\mathbf{S}[[\mathbf{D}, \mathbf{X}^{(1)}(\omega_1)], \mathbf{X}^{(2)}(\omega_2)]\mathbf{S} \\
&= \mathbf{V}[\mathbf{D}, \mathbf{X}^{(2)}(\omega_1, \omega_2)]_\mathbf{S}\mathbf{S} - \mathbf{S}[\mathbf{D}, \mathbf{X}^{(2)}(\omega_1, \omega_2)]_\mathbf{S}\mathbf{V}
\end{aligned}
\tag{26}
$$

To obtain the expressions above we have used the Fourier expansion of $X^{(1)}(t)$ (see Eq. (20)) and $X^{(2)}(t)$

$$
X^{(2)}(t) = \iint_{-\infty}^{\infty} \exp(-i(\omega_1 + \omega_1)t)X^{(2)}(\omega_1, \omega_2)d\omega \tag{27}
$$

Furthermore, we require the second order correction to be symmetric in the frequencies. The integration variables ω_1 and ω_2 have been symmetrized using the operator P_{12}, which creates the different permutations of the frequencies ω_1 and ω_2. Finally, using the definitions in Eq. (23)

and (24) along with

$$
\begin{aligned}
&\mathbf{E}^{[3]}\mathbf{X}^{(1)}(\omega_1)\mathbf{X}^{(1)}(\omega_2) = \\
&-\Bigg(\mathbf{G}(\frac{1}{2}[[\mathbf{D}, \mathbf{X}^{(1)}(\omega_1)], \mathbf{X}^{(2)}(\omega_2)]) \\
&\quad + \frac{1}{2}\mathbf{T}([\mathbf{D}, \mathbf{X}^{(1)}(\omega_1)]_\mathbf{S}, [\mathbf{D}, \mathbf{X}^{(1)}(\omega_2)]_\mathbf{S})\Bigg)\mathbf{DS} \\
&+ \mathbf{SD}\Bigg(\mathbf{G}(\frac{1}{2}[[\mathbf{D}, \mathbf{X}^{(1)}(\omega_1)], \mathbf{X}^{(2)}(\omega_2)]) \\
&\quad + \frac{1}{2}\mathbf{T}([\mathbf{D}, \mathbf{X}^{(1)}(\omega_1)]_\mathbf{S}, [\mathbf{D}, \mathbf{X}^{(1)}(\omega_2)]_\mathbf{S})\Bigg) \\
&- \mathbf{G}([\mathbf{D}, \mathbf{X}^{(1)}(\omega_1)]_\mathbf{S})[\mathbf{D}, \mathbf{X}^{(1)}(\omega_2)]_\mathbf{S}\mathbf{S} \\
&- \frac{1}{2}\mathbf{F}(\mathbf{D}_0)[[\mathbf{D}, \mathbf{X}^{(1)}(\omega_1)], \mathbf{X}^{(1)}(\omega_2)]\mathbf{S} \\
&+ \mathbf{S}[\mathbf{D}, \mathbf{X}^{(1)}(\omega_1)]_\mathbf{S}\mathbf{G}([\mathbf{D}, \mathbf{X}^{(1)}(\omega_2)]_\mathbf{S}) \\
&+ \frac{1}{2}\mathbf{S}[[\mathbf{D}, \mathbf{X}^{(1)}(\omega_1)], \mathbf{X}^{(1)}(\omega_2)]\mathbf{F}(\mathbf{D}_0)\mathbf{S}^{[3]}\mathbf{X}^{(1)}(\omega_1)\mathbf{X}^{(1)}(\omega_2)
\end{aligned}
\tag{28}
$$

and,

$$
\mathbf{S}^{[3]}\mathbf{X}^{(1)}(\omega_1)\mathbf{X}^{(1)}(\omega_2) = \frac{1}{2}\mathbf{S}[[\mathbf{D}, \mathbf{X}^{(1)}(\omega_1)], \mathbf{X}^{(2)}(\omega_2)]\mathbf{S} \tag{29}
$$

we obtain the well known form of the quadratic response equation

$$
\begin{aligned}
&(\mathbf{E}^{[2]} - (\omega_1 + \omega_2)\mathbf{S}^{[2]})\mathbf{X}^{(2)}(\omega_1, \omega_2) = \\
&\mathbf{V}[\mathbf{D}, \mathbf{X}^{(2)}(\omega_1, \omega_2)]_\mathbf{S}\mathbf{S} - \mathbf{S}[\mathbf{D}, \mathbf{X}^{(2)}(\omega_1, \omega_2)]_\mathbf{S}\mathbf{V} \\
&- P_{12}\left(\mathbf{E}^{[3]} - (\omega_1 + \omega_2)\mathbf{S}^{[3]}\right)\mathbf{X}^{(1)}(\omega_1)\mathbf{X}^{(1)}(\omega_2)
\end{aligned}
\tag{30}
$$

D.   Response Functions

Response functions describe the corrections to the expectation value of a Hermitian operator $\hat{A}$, representing an observable, due to the perturbation.

$$
\begin{aligned}
\langle\tilde{0}|\hat{A}|\tilde{0}\rangle &= \langle 0|\hat{A}|0\rangle \\
&+ \int_{-\infty}^{\infty} \langle\langle A; V(\omega)\rangle\rangle_\omega \exp[(-i\omega + \epsilon)t]d\omega \\
&+ \frac{1}{2}\iint_{-\infty}^{\infty} \langle\langle A; V(\omega_1), V(\omega_2)\rangle\rangle_{\omega_1, \omega_2} \\
&\qquad \exp[(-i(\omega_1 + \omega_2) + 2\epsilon)t]d\omega_1 d\omega_2 + ...
\end{aligned}
\tag{31}
$$

Using Eq. (10) to parametrize the expectation value

$$
\begin{aligned}
\text{Tr}(\mathbf{AD}(\mathbf{X})) &= \text{Tr}(\mathbf{AD}_0) + \text{Tr}(\mathbf{A}[\mathbf{D}, \mathbf{X}]_\mathbf{S}) \\
&+ \frac{1}{2}\text{Tr}(\mathbf{A}[[\mathbf{D}, \mathbf{X}], \mathbf{X}]) + \cdots
\end{aligned}
\tag{32}
$$

and the Fourier expansion of $\mathbf{X}$, collecting orders of the perturbation we obtain the linear response function

$$\langle\langle A; V(\omega)\rangle\rangle_\omega = \mathrm{Tr}(\mathbf{A}[\mathbf{D}, \mathbf{X}^{(1)}]_{\mathbf{S}}) \qquad (33)$$

and the quadratic response function

$$\begin{aligned}
\langle\langle A; V(\omega_1), V(\omega_2)\rangle\rangle_{\omega_1,\omega_2} &= \mathrm{Tr}(\mathbf{A}[\mathbf{D}, \mathbf{X}^{(2)}]_{\mathbf{S}}) \\
&+ \frac{1}{2}\mathrm{Tr}(\mathbf{A}[[\mathbf{D}, \mathbf{X}^{(1)}(\omega_1)], \mathbf{X}^{(1)}(\omega_2)]) \\
&+ \frac{1}{2}\mathrm{Tr}(\mathbf{A}[[\mathbf{D}, \mathbf{X}^{(1)}(\omega_2)], \mathbf{X}^{(1)}(\omega_1)])
\end{aligned} \qquad (34)$$

III. RESPONSE THEORY WITH APPROXIMATE INTEGRALS

When using an approximation like density-fitting the energy and Kohn-Sham matrix changes. This means that the Taylor expansion of the Kohn-Sham matrix must also change and a modified $\mathbf{G}$ and/or $\mathbf{T}$ of Eq. (15) and (16) is obtained. However, everything else remains the same. The response functions can still be evaluated from Eq. (33) and (34) with response parameters obtained by solving the response equations in Eq. (22) and Eq. (30). Excitation energies and excitation eigenvectors can still be determined from Eq. (25).

In this section we derive expressions for $\mathbf{G}$ and $\mathbf{T}$ for a number of popular approximations like density-fitting and the auxiliary density matrix method (ADMM). This framework is general and works for all approximations where the approximate Kohn-Sham matrix can be defined as the density matrix derivative of the approximate energy. This provides a clear roadmap for the implementation of response theory using both present and future approximations that accelerate the evaluation of contributions arising from the Coulomb and exchange integrals.

A. Kohn Sham matrix expansion using ADMM

The expression for the ADMM energy is based on the following trivial rearrangement of the total exchange energy (E^K);

$$E^K(\mathbf{D}) = E^k(\mathbf{d}) + E^K(\mathbf{D}) - E^k(\mathbf{d}), \qquad (35)$$

where $\mathbf{D}$ is the density matrix in the primary atomic-orbital (AO) basis and $\mathbf{d}$ is a density matrix obtained by projection of $\mathbf{D}$ to some (smaller) auxiliary AO basis, which represents an auxiliary electron density,

$$\rho_{\mathrm{admm}}(\mathbf{r}) = \sum_{\alpha\beta} \chi_\alpha(\mathbf{r})\chi_\beta(\mathbf{r})d_{\alpha\beta}. \qquad (36)$$

In the following we use upper-case letters to denote quantities evaluated in the primary basis, whereas lower-case letters refer to quantities in the auxiliary basis. The

ADMM exchange energy (E^K_{admm}) is obtained by replacing the exact-exchange terms $E^K(\mathbf{D}) - E^k(\mathbf{d})$ in Eq. (35) with exchange functionals $E^{\mathrm{admm}}_{\mathrm{xc}}[\rho] - E^{\mathrm{admm}}_{\mathrm{xc}}[\rho_{\mathrm{admm}}]$. Note, that the exchange functional used in the ADMM approximation (denoted with xc, admm) may be different from the exchange-correlation functional used (denoted with xc). The ADMM exchange energy is then,

$$\begin{aligned}
E^K_{\mathrm{admm}}(\mathbf{D}) &= E^k(\mathbf{d}) + E^{\mathrm{admm}}_{\mathrm{xc}}[\rho] - E^{\mathrm{admm}}_{\mathrm{xc}}[\rho_{\mathrm{admm}}] \\
&= \frac{1}{2}\sum_{\mu\rho\nu\sigma} d_{\mu\nu}(\mu\rho|\nu\sigma)d_{\rho\sigma} + \int_{\mathbb{R}^3} \epsilon_{\mathrm{x}}[\rho]\,\mathrm{d}\mathbf{r} \\
&- \int_{\mathbb{R}^3} \epsilon_{\mathrm{x}}[\rho_{\mathrm{admm}}]\,\mathrm{d}\mathbf{r}.
\end{aligned} \qquad (37)$$

We use indices $\mu, \nu, \rho, \sigma, \ldots$ for the primary AOs and indices $i, j, \ldots$ for occupied MOs expanded in the primary AOs. For auxiliary AOs greek letters are used $\alpha, \beta, \gamma, \delta, \ldots$ respectively.

Here we focus on the ADMM2 approximation where the projected density matrix $\mathbf{d}$ can be written in terms of the regular AO density matrix $\mathbf{D}$ as

$$\mathbf{d} = \mathbf{W}\mathbf{D}\mathbf{W}^T, \quad \mathbf{W} = \mathbf{s}^{-1}\mathbf{Q} \qquad (38)$$

Here $\mathbf{s}$ is the AO overlap matrix in the auxiliary basis with elements $s_{\alpha\beta} = \int \chi_\alpha(\mathbf{r}_1)\chi_\beta(\mathbf{r}_1)\mathrm{d}\mathbf{r}_1$; and $\mathbf{Q}$ is the mixed auxiliary-primary AO overlap matrix with elements $Q_{\alpha\mu} = \int \chi_\alpha(\mathbf{r}_1)\chi_\mu(\mathbf{r}_1)\mathrm{d}\mathbf{r}_1$

The ADMM2 exchange matrix is defined as

$$\begin{aligned}
K^{\mathrm{admm}}_{\mu\nu}(\mathbf{D}) &= \frac{\partial E^K_{\mathrm{admm}}}{\partial D_{\mu\nu}} \\
&= \mathbf{F}^{\mathrm{xc,admm}}_{\mu\nu}(\mathbf{D}) + \mathbf{W}^T(\mathbf{k}(\mathbf{d}) - \mathbf{f}^{\mathrm{xc,admm}}(\mathbf{d}))\mathbf{W}
\end{aligned} \qquad (39)$$

Its resulting derivatives can be expressed as

$$\begin{aligned}
\frac{\partial \mathbf{K}^{\mathrm{admm}}(\mathbf{D})}{\partial \mathbf{D}}\mathbf{M} &= \mathbf{K}^{\mathrm{xc,admm}}(\mathbf{M}) \\
&+ \mathbf{W}^T(\mathbf{k}(\mathbf{m}) - \mathbf{K}^{\mathrm{xc,admm}}(\mathbf{m}))\mathbf{W} \\
\frac{\partial^2 \mathbf{K}^{\mathrm{admm}}(\mathbf{D})}{\partial \mathbf{D}\partial \mathbf{D}}\mathbf{M}\mathbf{N} &= \mathbf{T}^{\mathrm{xc,admm}}(\mathbf{M}, \mathbf{N}) \\
&- \mathbf{W}^T(\mathbf{T}^{\mathrm{xc,admm}}(\mathbf{m}, \mathbf{n}))\mathbf{W}
\end{aligned} \qquad (40)$$

with

$$\mathbf{m} = \mathbf{W}\mathbf{M}\mathbf{W}^T \qquad \mathbf{n} = \mathbf{W}\mathbf{N}\mathbf{W}^T \qquad (41)$$

Due to the exchange-correlation contribution the exchange matrix will have contributions to all orders but here we limit ourself to quadratic response. Finally, the

ADMM2 approximation leads to the following expression

$$
\begin{aligned}
\mathbf{G}^{\mathrm{admm}}(\mathbf{M}) ={}& \mathbf{J}(\mathbf{M}) + w\mathbf{K}^{\mathrm{xc,admm}}(\mathbf{M}) \\
& + w\mathbf{W}^T(\mathbf{k}(\mathbf{m}) - \mathbf{K}^{\mathrm{xc,admm}}(\mathbf{m}))\mathbf{W} \\
& + \mathbf{K}^{\mathrm{xc}}(\mathbf{M}) \\
\mathbf{T}^{\mathrm{admm}}(\mathbf{M}, \mathbf{N}) ={}& w\mathbf{T}^{\mathrm{xc,admm}}(\mathbf{M}, \mathbf{N}) \\
& - w\mathbf{W}^T(\mathbf{T}^{\mathrm{xc,admm}}(\mathbf{m}, \mathbf{n}))\mathbf{W} + \mathbf{T}^{\mathrm{xc}}(\mathbf{M}, \mathbf{N})
\end{aligned}
$$
(42)

replacing Eq. (15) and (16).

B. Kohn Sham matrix expansion using density-fitting

In density fitting the products of two one-electron functions are expanded in auxiliary atom-centered functions $\alpha(\mathbf{r})$, according to

$$
|\mu\nu\rangle \approx |\widetilde{\mu\nu}\rangle = \sum_\alpha c_\alpha^{\mu\nu} |\alpha\rangle.
$$
(43)

The integrals $(\mu\nu|\rho\sigma)$ can be approximated in different ways, for example according to the three term expansion[14]

$$
(\mu\nu|\rho\sigma) \approx (\widetilde{\mu\nu|\rho\sigma}) = (\widetilde{\mu\nu}|\rho\sigma) + (\mu\nu|\widetilde{\rho\sigma}) - (\widetilde{\mu\nu}|\widetilde{\rho\sigma}), \quad (44)
$$

where the two first terms involve three-center integrals and the last term involves two-center integrals. The different flavours of density fitting arise from the choice of 1) the set of auxiliary functions $\{\alpha\}$ included in the expansion of Eq. (43), 2) how the fitting coefficients $c_\alpha^{\mu\nu}$ are obtained and 3) the ansatz for the integral approximation Eq. (44). The set of functions $\{\alpha\}$ can range from including only auxiliary functions centered on the two parent atoms[3] of μ and ν to the full set of auxiliary functions on all atoms in the molecule[4,5]. The fitting coefficients are obtained by minimizing the error $\Delta_{\mu\nu}^w$ of the residual density $|\delta_{\mu\nu}\rangle = |\mu\nu\rangle - |\widetilde{\mu\nu}\rangle$ in metric w

$$
\Delta_{\mu\nu}^w = \langle \delta_{\mu\nu}|w|\delta_{\mu\nu}\rangle
$$
(45)

where w can range[11,13] from the Coulomb operator r_{12}^{-1} to the Dirac delta function (overlap metric fitting), and where the minimization can be subjected to charge, dipole or higher-order constraints. The three term ansatz of Eq. (44) is denoted *robust*[14] in the sense that it ensures that the errors in the fitted integrals are bilinear with respect to the errors in the two-center fits,

$$
(\mu\nu|\rho\sigma) - (\widetilde{\mu\nu|\rho\sigma}) = (\delta_{\mu\nu}|\delta_{\rho\sigma}),
$$
(46)

whereas including for instance only the first term has a linear error. We note that when doing the standard (unconstrained) Coulomb-metric fitting over the full set of auxiliary functions, giving the *fitting* equation set

$$
\sum_\beta (\alpha|\beta)c_\beta^{\mu\nu} = (\alpha|\mu\nu),
$$
(47)

and similarly for $|\rho\sigma)$, the error is bilinear using only the first (or second) term of Eq. (44), as it follows from Eq. (47) that $(\widetilde{\mu\nu}|\rho\sigma) = (\mu\nu|\widetilde{\rho\sigma}) = (\widetilde{\mu\nu}|\widetilde{\rho\sigma})$, and thus the second and third (or the first and third) terms of Eq. (44) cancel.

When considering external perturbations, one needs to include Lagrangian terms in the integral approximation to ensure that the equations for the fitting coefficients are satisfied with respect to the perturbation. In this paper we only consider perturbations that do not affect the fitted integrals, and the Lagrangian formalism therefore does not need to be considered here. Hence, the application of response theory is straightforwardly achieved by a simple replacement of the exact integrals $(\mu\nu|\rho\sigma)$ with the fitted integrals $(\widetilde{\mu\nu|\rho\sigma})$. For the standard density-fitting approximation we simply replace the exact expressions of $J(\mathbf{M})$ and $K(\mathbf{M})$ in Eq. (15), with the approximate expressions $\tilde{J}(\mathbf{M})$ and $\tilde{K}(\mathbf{M})$, given by

$$
\begin{aligned}
\tilde{J}(\mathbf{M}) &= \sum_{\rho\sigma} (\widetilde{\mu\nu|\rho\sigma}) M_{\rho\sigma} = \sum_\alpha (\mu\nu|\alpha)c_\alpha, \\
\tilde{K}(\mathbf{M}) &= \sum_{\rho\sigma} (\widetilde{\mu\sigma|\rho\nu}) M_{\rho\sigma} = \sum_\alpha \sum_{\rho\sigma} (\mu\sigma|\alpha)c_\alpha^{\rho\nu} M_{\rho\sigma}, \\
c_\alpha &\equiv \sum_{\rho\sigma} c_\alpha^{\rho\sigma} M_{\rho\sigma} = (\alpha|\beta)^{-1} \sum_{\rho\sigma} (\beta|\rho\sigma) M_{\rho\sigma},
\end{aligned}
$$
(48)

to obtain

$$
\tilde{\mathbf{G}}(\mathbf{M}) = \tilde{\mathbf{J}}(\mathbf{M}) + w \cdot \tilde{\mathbf{K}}(\mathbf{M}) + \mathbf{K}^{\mathrm{xc}}(\mathbf{M}).
$$
(49)

We note that approximate Fock/KS matrix construction that requires a decomposition of the density matrix (such as using (local) molecular orbitals[29,80]) cannot straightforwardly be applied as the density matrix dependence changes with the external perturbation. Similarly, certain linear scaling density-fitting approximations have an explicit dependence on the density.

C. Kohn Sham matrix expansion using COSX

Although we do not use COSX in this paper, we include it here as an additional example of an alternative approach that may be accommodated in this framework. Similar to the pseudo-spectral method[38–40] the COSX algorithm evaluates ERIs using a semi-numerical approximation[37,81], where one of the two electronic coordinate integrations are performed on a grid and where the other integration is performed analytically. The exchange energy is given by

$$
E^{K,\mathrm{COSX}} = D_{\mu\nu} X_{\mu g} A_{\nu\sigma}(\mathbf{r}_g) D_{\rho\sigma} X_{\lambda g}
$$
(50)

with $X_{\lambda g} = \sqrt{w_g}\chi_\lambda(\mathbf{r}_g)$, w_g the grid weight, and $A_{\nu\sigma} = \int \chi_\nu(\mathbf{r})\chi_\sigma(\mathbf{r})|\mathbf{r}-\mathbf{r}_g|^{-1}d\mathbf{r}$. The COSX exchange matrix is

defined as the density matrix derivative of the exchange energy.

$$K_{\mu\nu}^{\text{COSX}} = \frac{\delta E^{K,\text{COSX}}}{\delta D_{\mu\nu}} = X_{\mu g} A_{\nu\sigma}(\mathbf{r}_g) D_{\rho\sigma} X_{\lambda g} \quad (51)$$

The COSX exchange matrix has the same density matrix dependence as the regular exchange matrix

$$\left. \frac{\partial \mathbf{K}_{\mu\nu}^{\text{COSX}}}{\partial \mathbf{D}(\mathbf{X})} \right|_{\mathbf{D}(\mathbf{X})=\mathbf{D}_0} \mathbf{M} = \mathbf{K}_{\mu\nu}^{\text{COSX}}(\mathbf{M}) \quad (52)$$

while all higher order contributions vanish. Finally, we obtain

$$\mathbf{G}^{\text{COSX}}(\mathbf{M}) = \mathbf{J}(\mathbf{M}) + w \cdot \mathbf{K}^{\text{COSX}}(\mathbf{M}) + \mathbf{K}^{\text{xc}}(\mathbf{M}) \quad (53)$$

to replace the Eq. (15).

IV. COMPUTATIONAL DETAILS

The accuracy of the density fitting and ADMM approximations has been tested on a set of 11 molecules for electronic ground state energies, vertical excitation energies, static polarizabilities and first hyperpolarizabilities. For the vertical excitation energies, the five lowest excitations were considered. Oscillator strengths are reported in the supplementary information.

The test set of small to medium sized molecules has been chosen from Ref. 82. The molecules investigated are acetamide (C_2H_5ON), acetone (C_3H_6O), butadiene (C_4H_6), cyclopropene (C_3H_4), ethene (C_2H_4), formaldehyde (CH_2O), formamide (CH_3ON), furan (C_4H_4O), imidazole ($C_3H_4N_2$), propanamide (C_3H_7ON) and pyrrole (C_4H_5N). This set of molecules will in the following be denoted as M11.

The methods under investigation have been run with a local development version of LSDalton[83,84] on single nodes of a 2.6 GHz Intel E5-2670 cluster, employing OpenMP to utilize the 16 cores on each node. The DFT functional CAM-B3LYP[85] has been employed using the specifications α=0.21, β=0.79 and μ=0.45. This choice has been taken in order to have full long-range exchange treatment, as needed in particular for polarizabilities and first hyperpolarizabilities, and also for some of the investigated excitation energies.

For each property, the basis set performance of three different types of calculations labelled as *full*, *df-J* and *admm* have been investigated. Here "full" are regular calculations employing standard J-engine techniques[32–34] for the Coulomb contribution and LinK[86] for the exchange contribution, i.e. without any approximation (except standard acceleration techniques and integral prescreening), "df-J" refers to the combination of density-fitting for Coulomb and LinK for exchange, and "admm" to the combination of density-fitting for Coulomb and ADMM (ADMM2) for exchange.

For the basis set performance, we have chosen the Jensen DFT optimized optimized pcseg-n and aug-pcseg-n basis sets[87] as orbital basis, and have investigated the accuracy for cardinal numbers $n = 1, 2, 3$ against reference aug-pcseg-4 calculations. The prefix "aug" indicates the use of augmented functions. For density-fitting the Karlsruhe def2-QZVPP auxiliary basis set of Weigend has been employed[88], for pcseg-n ADMM calculations the admm-n basis sets[89] have been employed, and for aug-pcseg-n ADMM calculations aug-admm-n bases have been employed. These admm-n basis sets have been specifically optimized for the ADMM approximation to be used along with the pcseg-n and family of basis sets, and the aug-admm-n basis sets have been adapted by augmenting the admm-n basis sets using the augmented function from the aug-pcseg-n basis sets with cardinal number $n - 1$. For details on the admm-n basis sets see Ref. 89.

V. RESULTS AND DISCUSSION

Rather than investigating the errors of each method in a given basis set, we have here chosen to make a comparison against the basis set limit. This choice has been taken in order to assess how the methods perform in typical practical calculations. In the following a graphical summary is presented, visualizing normal distributions

$$f(x) = N exp(-\frac{(x-\mu)^2}{2\sigma^2}) \quad (54)$$

using the mean error μ and the standard deviation σ for each employed approximation, property and basis set. The normalization N has been chosen to make the differences among methods and basis sets visually more accessible; for electronic ground-state energies we have used the normalization $N = \log(\frac{1}{\sqrt{2\sigma^2\pi}})$, and for excitation energies, isotropic polarizabilities, anisotropic polarizabilties and dipolehyperpolarizabilty $N = \frac{1}{\sqrt[4]{2\sigma^2\pi}}$. For the figures we have chosen to represent only the "df-J" and "admm" results, since the "full" and "df-J" results are virtually identical. We refer the reader instead to the supporting information for detailed results including all three types of calculations. In the figures, the labels "df-J n" and "admm n" denote a df-J and admm type calculation, respectively, employing the pcseg-n basis sets, and similarly "df-J aug-n" and "admm aug-n" where the aug-pcseg-n basis sets are employed. Please note that throughout we used capital letter ADMM for the ADMM approximation and lower case letters admm for the calculations using both df-J and ADMM.

A. Electronic ground-state energy

In Figure 1 the normal distributions of the errors in electronic ground-state energy per electron for pcseg-n,
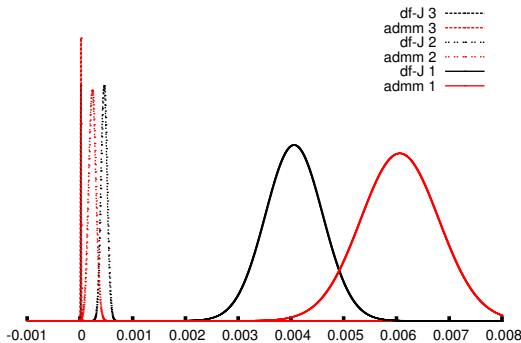
FIG. 1. The normal distribution of errors in the molecular ground state energy (in atomic units) with CAM-B3LYP (α=0.21,β=0.79,μ=0.45)/pcseg-n (n=1, 2, 3) for a set of molecules M11 (see text). Here aug-pcseg-4 results are taken as the reference.

FIG. 2. The normal distribution of errors in the molecular ground state energy (in atomic units) with CAM-B3LYP (α=0.21,β=0.79,μ=0.45)/aug-pcseg-n (n=1, 2, 3) for a set of molecules M11 (see text). Here aug-pcseg-4 results are taken as the reference.

$n = 1, 2, 3$, in reference to aug-pcseg-4, are plotted for df-J and admm calculations. We emphasise again that the full and the df-J results are very similar and we have therefore chosen to present only one of the two in the plots. The results for all three methods are given in the supplementary information Table **??**. Some representative example numbers are presented and discussed in the text below.

While the variance (width) is rather large for both methods when a pcseg-1 basis set is employed a clear improvement is seen upon increasing the basis set to pcseg-2 and pcseg-3; the errors are reduced by about one order of magnitude with each cardinal number n, for all methods. On average all methods investigated overestimate the ground state energy compared to the aug-pcseg-4 reference, which is to be expected from any variational approach. For example, the mean errors (standard deviations) in a pcseg-2 basis are 458(58), 456(58) and 232(69) μE_H for full, df-J and admm type calculations, respectively, while for pcseg-3 basis these values decrease to 17(2), 14(2) and 21(6) μE_H; all of which are well below 1 kcal/mol (or 1594 μE_H). Although the mean error for admm at the pcseg-2 level is smaller than for the df-J calculation by almost a factor two, it is about 50% larger in the other two cases, and the standard deviation for admm is larger in each case.

In Figure 2 the corresponding errors in the electronic ground-state energies are depicted for aug-pcseg-n, $n = 1, 2, 3$. As expected, augmentation leads to some improvement (reducing the errors by $10 - 30\%$), but does not change the observed trends.

B. Vertical excitation energies

Figures 3 and 4 show the normal distributions of the absolute errors in the five lowest vertical excitation energies of the M11 benchmark set for df-J and admm type
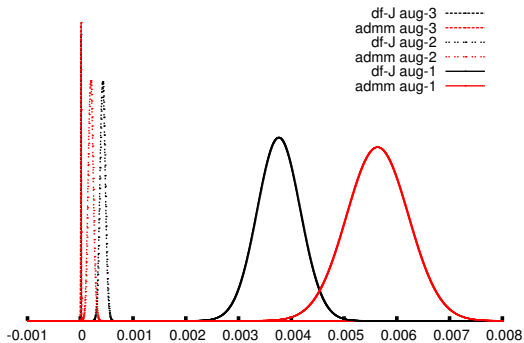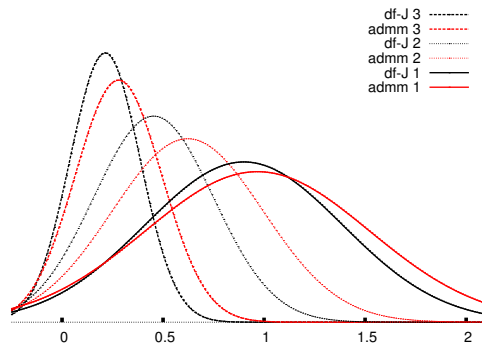

FIG. 3. The normal distribution of errors in the first five excitation energies (in electron volt) with CAM-B3LYP(α=0.21,β=0.79,μ=0.45)/pcseg-n (n=1, 2, 3) for a set of molecules M11 (see text). Here aug-pcseg-4 results are taken as the reference.

calculations using pcseg-n and aug-pcseg-n basis sets, with $n = 1, 2, 3$, respectively. The 55 excitation energies considered here are in the range 3.93 eV to 8.96 eV at the reference aug-pcseg-4 full level of theory. The calculations have been run without any point group symmetry, and no attempt has been made to identify the different states. Thus, the order of the excitation energies may vary, in particular for nearly degenerate states, at different basis set and theory levels.

Similar to the trend for the electronic ground-state energies, the excitation energies are overestimated as compared to the aug-pcseg-4 reference. All methods show a systematic improvement with increasing cardinal number n, and at each level n, the full and df-J type calculations perform better than admm. Upon augmentation the errors get reduced by one to two orders of magnitude, and already at the aug-pcseg-1 basis set level the errors are smaller that the corresponding pcseg-3 results; with er-
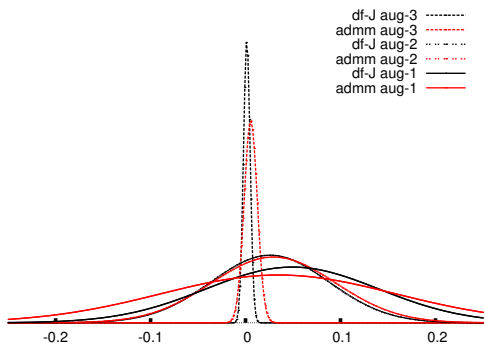
FIG. 4. The normal distribution of errors in the first five excitation energies (in electron volt) with CAM-B3LYP(α=0.21,β=0.79,μ=0.45)/aug-pcseg-n (n=1, 2, 3) for a set of molecules M11 (see text). Here aug-pcseg-4 results are taken as the reference.

FIG. 5. The normal distribution of error in the isotropic polarizability (in atomic units) with CAM-B3LYP(α=0.21,β=0.79,μ=0.45)/pcseg-n (n=1, 2,3) for a set of molecules M11 (see text). Here aug-pcseg-4 results are taken as the reference.

rors 49(91) meV, 49(91) meV and 34(124) meV, for full, df-J and admm type calculations, respectively. Standard deviations are given in parenthesis. This is already within the range of typical TD-DFT excitation errors, of about 0.1 eV or larger (see for instance Ref. 90). For aug-pcseg-2 the standard deviations are reduced by another $32 - 47\%$, and by roughly an order of magnitude further by going to aug-pcseg-3. See supplementary information Table **??** for details.

C. Static polarizabilities

The normal distribution of the errors in static isotropic polarizabilties at the CAM-B3LYP (α=0.21, β=0.79 and μ=0.45) level for the M11 benchmark is depicted in Figures 5 and 6, for pcseg-n and aug-pcseg-n with $n = 1, 2, 3$, respectively. The isotropic polarizabilities are underestimated in all basis sets and at all levels of theory, with a clear improvement for increasing cardinal number n and upon augmentation. The full numbers are given in Table **??** in the supplementary information. At the reference aug-pcseg-4 full level of theory, the isotropic polarizabilities of the M11 benchmark range from 27.5 to 55.7 a.u. (1 a.u. equals $(0.529\text{Å})^3 = 0.148\text{Å}^3$). At the pcseg-1 level the mean errors (standard deviations) are $-6.96(2.70)$, $-6.96(2.70)$ and $-7.32(2.88)$ a.u. for full, df-J and admm type calculations, respectively, and the errors are reduced by roughly an order of magnitude, to $-0.50(0.20)$, $-0.50(0.20)$ and $-0.84(0.33)$ a.u., at the pcseg-3 level. Upon augmentation the errors are reduced by one to three orders of magnitude. Already at the aug-pcseg-1 basis the errors are $-0.31(0.12)$, $-0.31(0.12)$ and $-1.03(0.45)$, whereas at aug-pcseg-3 they as low as $-3(1)$, $-1(3)$ and $-12(5)$ ma.u. With typical DFT errors ranging from 0.2 to 1.0 a.u., see for instance Ref. 91, basis sets errors are at an acceptable level from the aug-pcseg-2 level of theory, for all three levels of theory, and
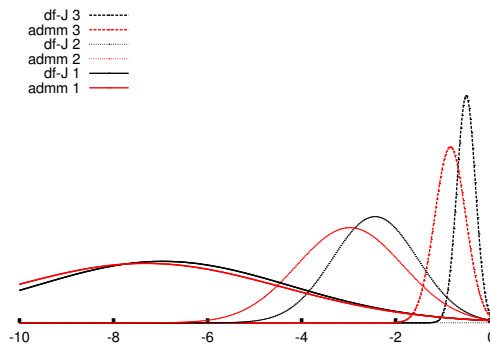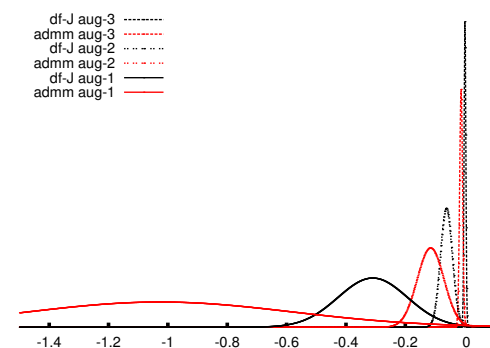

FIG. 6. The normal distribution of error in the isotropic polarizability (in atomic units) with CAM-B3LYP(α=0.21,β=0.79,μ=0.45)/aug-pcseg-n (n=1, 2,3) for a set of molecules M11 (see text). Here aug-pcseg-4 results are taken as the reference.

remaining basis set errors are essentially removed upon using the aug-pcseg-3 basis set. The admm type calculations have larger errors in all cases, by up to a factor 4 at the aug-pcseg-1 level, and for the aug-pcseg-n basis the admm errors more or less bisect the values of the full (and df-J) calculations of cardinal numbers $n-1$ and n.

The error distributions for the static anisotropic polarizabilities are shown in Figures 7 and 8. For the M11 benchmark the anisotropic polarizabilities range from 8.0 to 47.0 a.u. at the reference aug-pcseg-4 full level of theory. Although the mean errors are typically slightly smaller than for the isotropic polarizabilities, the standard deviations are larger; as an example the errors are $-0.23(0.35)$, $-0.24(0.36)$ and $-0.38(0.67)$ a.u. for aug-pcseg-1 and $-2(3)$, $-8(9)$ and $-21(25)$ ma.u. for aug-pcseg-3; see Table **??** in the supplementary information for the full list of mean errors and standard deviations. Similar to the isotropic polarizability, the anisotropic po-
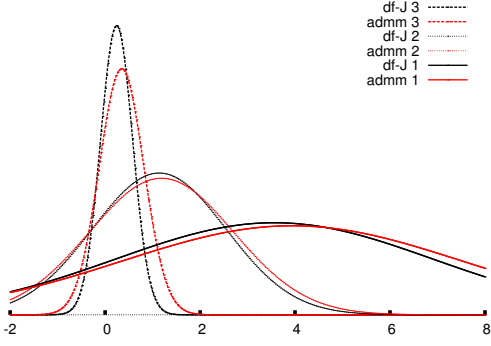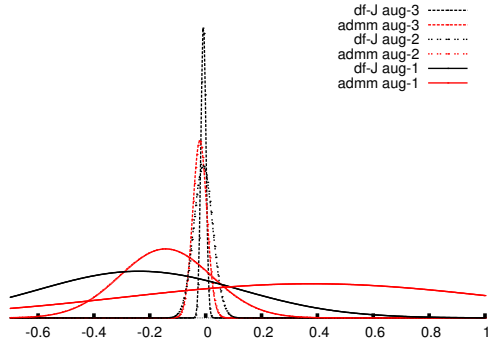
FIG. 7. The normal distribution of error in the anisotropic polarizability (in atomic units) with CAM-B3LYP(α=0.21,β=0.79,μ=0.45)/pcseg-n (n=1, 2,3) for a set of molecules M11 (see text). Here aug-pcseg-4 results are taken as the reference.

FIG. 9. The normal distribution of error in the BetaParallel (firsthyperpolarizability) (in atomic units) with CAM-B3LYP(α=0.21,β=0.79,μ=0.45)/pcseg-n (n=1, 2,3) for a set of molecules M11 (see text). Here aug-pcseg-4 results are taken as the reference.

FIG. 8. The normal distribution of error in the anisotropic polarizability (in atomic units) with CAM-B3LYP(α=0.21,β=0.79,μ=0.45)/aug-pcseg-n (n=1, 2,3) for a set of molecules M11 (see text). Here aug-pcseg-4 results are taken as the reference.

FIG. 10. The normal distribution of error in the BetaParallel (firsthyperpolarizability) (in atomic units) with CAM-B3LYP(α=0.21,β=0.79,μ=0.45)/aug-pcseg-n (n=1, 2,3) for a set of molecules M11 (see text). Here aug-pcseg-4 results are taken as the reference.

larizabilities are underestimated using aug-pcseg-n basis, with the exception of aug-pcseg-1 admm type calculations. For the pcseg-n basis, the values are instead overestimated. As for the isotropic polarizabilities the admm aug-pcseg-n errors fall in between the aug-pcseg-$(n-1)$ and aug-pcseg-n full errors, although shifted towards the aug-pcseg-$(n-1)$ values, indicating that admm provides a somewhat poorer description of the directional components.

D. Static hyperpolarizabilities

To assess how the methods perform for the first hyperpolarizability we have here chosen to study the component of the dipole first hyperpolarizability tensor $\bar{\beta}$ along the direction of the permanent molecular dipole moment
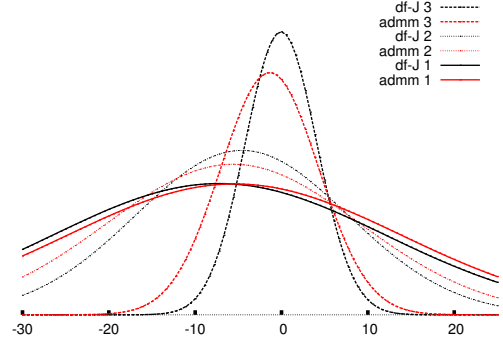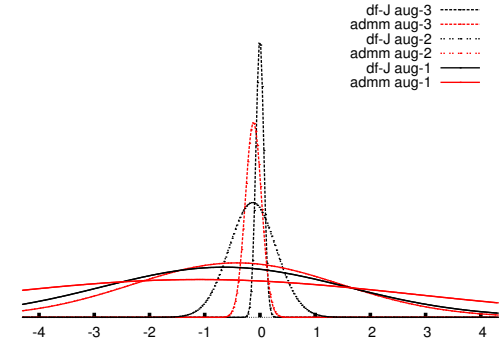
$\boldsymbol{\mu} = (\mu_x, \mu_y, \mu_z)$, given by[92,93]

$$\bar{\beta} = \frac{3}{5|\mu|} \left(\beta_x\mu_x + \beta_y\mu_y + \beta_z\mu_z\right), \qquad (55)$$

with

$$\beta_\xi = \sum_{\zeta=x,y,z} \beta_{\xi\zeta\zeta}, \quad \xi = x,y,z, \qquad (56)$$

where $\beta_{\xi\zeta\gamma}$ are components of the static first hyperpolarizability tensor. Figures 9 and 10 show the normal distribution of CAM-B3LYP(α=0.21,β=0.79,μ=0.45) errors in the static dipole hyperpolarizability $\bar{\beta}$ for the M11 benchmark, for pcseg-n and aug-pcseg-n, $n = 1, 2, 3$, calculations, respectively, and full results are provided in Tables **??** of the supplementary information.

At the reference aug-pcseg-4 full calculation the parallel values vary from -41.6 to 15.3 a.u. The standard deviations in the pcseg-n basis are rather large, and vary

TABLE I. Average wall timings in seconds per SCF iteration for the acetone molecule, for 'full', 'df-J' and 'admm' type calculations (see text for further details).

Method type	aug-pcseg-1	aug-pcseg-2	aug-pcseg-3
full	4.1	49	590
df-J	3.9	43	491
admm	3.2	13	73

from 19.3 a.u. for $n = 1$ to 4.1 a.u. for $n = 3$, for both df-J and full type calculations, and 19.4 to 5.7 a.u. for admm type calculations. Upon augmentation the standard deviations are reduced to the ranges 2.2 to 0.05 a.u. for full, 2.2 to 0.07 a.u. for df-J and 3.9 to 0.15 for admm type calculations. In all cases the admm-n results falls in between the df-J-n and df-J-$(n-1)$ results; for pcseg-n the admm results are shifted toward n, and for aug-pcseg-n the results are less conclusive with the aug-pcseg-2 admm result close to the aug-pcseg-1 full value and the aug-pcseg-3 admm result slightly shifted towards the aug-pcseg-3 full result.

E. Performance

In the previous subsections we have presented results for electronic ground-state energies, the first five excitation energies, polarizabilities and first hyperpolarizabilities for the M11 benchmark set. The results show that density-fitting for the Coulomb contribution has negligible effects on the results, and that employing ADMM for the exchange can be done in a systematic fashion, albeit at the cost of slightly reduced accuracy. In this section we give our assessment of performance versus accuracy for an example molecule, to provide an indicative guide to choosing which method to use in an practical calculations.

Averaged timings per SCF iteration for the three different types of calculation (full, df-J and admm) are given in Table I, for aug-pcseg-n calculations on the acetone molecule, which is on the median of the 11 molecules with regards to computational time. The timings for the response part of the calculation are similar, and we refer the interested reader to the supporting information Table **??** which includes timings for the individual components for both SCF and the response parts of the calculation. In Table I full-type calculations are the sum of reg-J, LinK, XC and solver timings of Supporting Information Table **??**, df-J type calculations the sum of df-J, LinK, XC and solver timings, and admm type calculations the sum of df-J, ADMM, XC and solver.

The performance gains using density-fitting are tremendous when looking at the effect on the Coulomb contribution alone, with speed up factor 7, 27 and 112 for aug-pcseg-n, with cardinal number $n = 1, 2, 3$ respectively. As shown, this performance boost can be attained at little to no loss in accuracy, and density fitting can be

applied without hesitation. However, for the hybrid DFT calculations presented here, these speed ups have limited effect on the total timings, with only 5%, 12% and 17% reduction in computational time for the aug-pcseg-n sequence, with $n = 1, 2, 3$ respectively. This is because LinK exchange is the main bottleneck for these calculations, amounting for df-J type calculations to 67%, 85% and 95% of the total wall time, for $n = 1, 2, 3$.

The motivation to enhance the performance of the exchange contribution should be clear from these results, and the ADMM approximation gives significant speed ups. For the aug-pcseg-n sequence the speed up for the exchange contribution is factor 1.5, 5.8 and 9.7, for $n = 1, 2, 3$, respectively. Whilst these speedups are significantly less than those obtained for the Coulomb term using density-fitting, the combined performance gain using both density fitting for Coulomb and ADMM for exchange is worthwhile with overall speedup factors of 1.2, 3.7 and 8.1. However, these speedups come at a cost of accuracy, mainly due to the ADMM approximation. For electronic ground-state energies, the effect on accuracy due to ADMM is minimal, and the performance gains of ADMM and density fitting outweigh the small loss in accuracy. For excitation energies the same arguments hold, although the speed ups when calculating five excitation energies (as done in this paper) are somewhat smaller than for the ground-state energies.

For polarizabilities and hyperpolarizabilities the results are less clear-cut. For the calculation of isotropic polarizabilities ADMM gives a fairly good description still, whereas for the anisotropic polarizabilities this is no longer the case. For hyperpolarizabilities the admm aug-pcseg-3 results reduce the standard deviation of the full aug-pcseg-2 results by a factor 2.9 and the additional computational time is only factor 1.5. Going to the full aug-pcseg-3 the standard deviation is reduced by an additional factor 3.0, now for a factor 8.1 in computational time. Clearly the admm aug-pcseg-3 type calculation is a valid and efficient option. This does not hold for admm aug-pcseg-2 however. Going from full aug-pcseg-1 reduces the standard deviation by factor 1.2 for an increase in computational time by factor 3.2. Using instead the full aug-pcseg-2 reduces the error by factor 4.5 for a cost of factor 3.7 in calculation time.

In summary, the presented results indicate that density fitting of the Coulomb contribution can be used without hesitation for all properties studied here, although the overall performance gains for hybrid functionals are limited by the efficiency of the exchange contribution. The ADMM exchange approximation can readily be applied for ground-state and excitation energies, whereas for polarizabilities and hyperpolarizabilities the accuracy to performance ratio is more questionable.

VI. SUMMARY AND CONCLUSIONS

We have presented an extension to the standard formulation of response theory, which accounts for approximate Fock/Kohn-Sham matrices such as the matrices used in density-fitting or the ADMM2 approximation. The development represents a framework to easily introduce the approximate methodologies used in ground-state electronic structure calculations to Hartree-Fock/Kohn-Sham response theory, provided that the Coulomb and exchange matrices can be formulated as derivatives of the approximated Coulomb and Exchange energies.

The option for the combined use of density-fitting and ADMM has been implemented and tested in the LSDalton program[84]. An error analysis with respect to different basis sets and the new combined approximations has been performed for DFT ground state energies, vertical excitation energies, static polarizabilities and hyperpolarizabilities for a set of 11 small to medium sized molecules.

The presented results indicate that density fitting of the Coulomb contribution can be used without hesitation for all properties studied here, although the overall performance gains for hybrid functionals are limited by the treatment of the exchange contribution. The ADMM exchange approximation can be applied to accelerate the evaluation of the exchange contribution, although this entails introducing additional approximations. The ADMM approach was found to work well for ground-state and excitation energies, whereas for polarizabilities and hyperpolarizabilities the accuracy to performance ratio is less favourable, indicating the need for care when applying it to new molecular response properties.

VII. ACKNOWLEDGMENT

[1] J. L. Whitten, "Coulombic potential energy integrals and approximations," J. Chem. Phys. **58**, 4496–4501 (1973).

[2] J. A. Jafri and J. L. Whitten, "Electron repulsion integral approximations and error bounds: Molecular applications," J. Chem. Phys. **61**, 2116–2121 (1974).

[3] E. J. Baerends, D. E. Ellis, and P. Ros, "Self-consistent molecular Hartree–Fock–Slater calculations. I. The computational procedure," Chem. Phys. **2**, 41–51 (1973).

[4] B. I. Dunlap, J. W. D. Connolly, and J. R. Sabin, "On some approximations in applications of X_α theory," J. Chem. Phys. **71**, 3396–3402 (1979).

[5] B. I. Dunlap, J. W. D. Connolly, and J. R. Sabin, "On first–row diatomic molecules and local density models," J. Chem. Phys. **71**, 4993–4999 (1979).

[6] O. Vahtras, J. Almlöf, and M. W. Feyereisen, "Integral approximations for LCAO-SCF calculations," Chem. Phys. Lett. **213**, 514–518 (1993).

[7] F. Neese, "An Improvement of the Resolution of the Identity Approximation for the Formation of the Coulomb Matrix," J. Comput. Chem. **24**, 1740–1747 (2003).

[8] S. Reine, A. Krapp, M. F. Iozzi, V. Bakken, T. Helgaker, F. Pawłowski, and P. Sałek, "An efficient density-functional-theory force evaluation for large molecular systems," J. Chem. Phys. **133**, 044102 (2010).

[9] F. Weigend, "A fully direct RI-HF algorithm: Implementation, optimised auxiliary basis sets, demonstration of accuracy and efficiency," Phys. Chem. Chem. Phys. **4**, 4285–4291 (2002).

[10] R. Polly, H.-J. Werner, F. R. Manby, and P. J. Knowles, "Fast hartree-fock theory using local density fitting approximations," Mol. Phys. **102**, 2311–2321 (2004).

[11] A. Sodt, J. E. Subotnik, and M. Head-Gordon, "Linear scaling density fitting," J. Chem. Phys. **125**, 194109 (2006).

[12] A. Sodt and M. Head-Gordon, "Hartree-fock exchange computed using the atomic resolution of the identity approximation," J. Chem. Phys. **128**, 104106 (2008).

[13] S. Reine, E. Tellgren, A. Krapp, T. Kjærgaard, T. Helgaker, B. Jansík, S. Høst, and P. Sałek, "Variational and robust density fitting of four-center two-electron integrals in local metrics." J. Chem. Phys. **129**, 104101 (2008).

[14] B. I. Dunlap, "Robust variational fitting: Gaspar's variational exchange can accurately be treated analytically," J. Mol. Struct. (Theochem) **501**, 221–228 (2000).

[15] P. Merlot, T. Kjærgaard, T. Helgaker, R. Lindh, F. Aquilante, S. Reine, and T. B. Pedersen, "Attractive electron–electron interactions within robust local fitting approximations," J. Comput. Chem. **34**, 1486 (2013).

[16] D. S. Hollman, H. F. Schaefer, and E. F. Valeev, "Semi-exact concentric atomic density fitting: reduced cost and increased accuracy compared to standard density fitting." J. Chem. Phys. **140**, 064109 (2014).

[17] F. Weigend and R. Ahlrichs, "Balanced basis sets of split valence, triple zeta valence and quadruple zeta valence quality for H to Rn: Design and assessment of accuracy." Phys. Chem. Chem. Phys. **7**, 3297–3305 (2005).

[18] F. Weigend, "Hartree–Fock exchange fitting basis sets for H to Rn," J. Comp. Chem. **29**, 167–175 (2008).

[19] S. F. Manzer, E. Epifanovsky, and M. Head-Gordon, "Efficient Implementation of the Pair Atomic Resolution of the Identity Approximation for Exact Exchange for Hybrid and Range-Separated Density Functionals," J. Chem. Theory Comput. **15**, 518–527 (2015).

[20] S. Manzer, P. R. Horn, N. Mardirossian, and M. Head-Gordon, "Fast, accurate evaluation of exact exchange: The occ-RI-K algorithm," J. Chem. Phys. **143**, 024113 (2015).

[21] F. R. Manby, "Density fitting in second-order linear-r12 møller-plesset perturbation theory," J. Chem. Phys. **119**, 4607–4613 (2003).

[22] M. Feyereisen and G. Fitzgerald, "Use of approximate integrals in ab initio theory. an application in mp2 energy calculations," Chem. Phys. Lett. **208**, 359–363 (1993).

[23] H.-J. Werner, F. R. Manby, and P. J. Knowles, "Fast linear scaling second-order Møller-Plesset perturbation theory (MP2) using local and density fitting approximations," J. Chem. Phys. **118**, 8149–8160 (2003).

[24] H.-J. Werner and F. R. Manby, "Explicitly correlated second-order perturbation theory using density fitting and local approximations," J. Chem. Phys. **124**, 054114 (2006).

[25] H. Eshuis, J. Yarkony, and F. Furche, "Fast computation of molecular random phase approximation correlation energies using resolution of the identity and imaginary frequency integration," J. Chem. Phys. **132**, 234114 (2010).

[26] X. Ren, P. Rinke, V. Blum, J. Wieferink, A. Tkatchenko, A. Sanfilippo, K. Reuter, and M. Scheffler, "Resolution-of-identity approach to Hartree-Fock, hybrid density functionals, RPA, MP2 and GW with numeric atom-centered orbital basis functions," New J. Phys. **14**, 053020 (2012).

[27] N. H. F. Beebe and J. Linderberg, "Simplifications in the generation and transformation of two-electron integrals in molecular calculations," Int. J. Quantum Chem. **12**, 683–705 (1977).

[28] H. Koch, A. Sánchez de Merás, and T. B. Pedersen, "Reduced scaling in electronic structure calculations using Cholesky decompositions," J. Chem. Phys. **118**, 9481–9484 (2003).

[29] F. Aquilante, T. B. Pedersen, and R. Lindh, "Low-cost evaluation of the exchange fock matrix from cholesky and density fitting representations of the electron repulsion integrals," J. Chem. Phys. **126**, 194106 (2007).

[30] T. B. Pedersen, F. Aquilante, and R. Lindh, "Density fitting with auxiliary basis sets from cholesky decompositions," Theor. Chem. Acc. **124**, 1–10 (2009).

[31] F. Aquilante, L. Boman, J. Boström, H. Koch, R. Lindh, A. Sánchez de Merás, and T. B. Pedersen, "Cholesky Decomposition Techniques in Electronic Structure Theory," in *Linear-Scaling Techniques in Computational Chemistry and Physics. Methods and Applications*, Challenges and Advances in Computational Chemistry and Physics, Vol. 13, edited by R. Zalesny, M. G. Papadopoulos, P. G. Mezey, and J. Leszczynski (Springer, 2011) Chap. 13, pp. 301–343.

[32] G. R. Ahmadi and J. Almlöf, "The coulomb operator in a gaussian product basis," Chem. Phys. Lett. **246**, 364 (1995).

[33] C. A. White and M. Head-Gordon, "A j matrix engine for density functional theory calculations," J. Chem. Phys. **104**, 2620 (1996).

[34] Y. Shao and M. Head-Gordon, "An improved j matrix engine for density functional theory calculations," Chem. Phys. Lett. **323**, 425 – 433 (2000).

[35] M. Guidon, J. Hutter, and J. VandeVondele, "Auxiliary density matrix methods for hartree–fock exchange calculations," J. Chem. Theory Comput. **6**, 2348–2364 (2010).

[36] P. Merlot, R. Izsák, A. Borgoo, T. Kjærgaard, T. Helgaker, and S. Reine, "Charge-constrained auxiliary-density-matrix methods for the hartree–fock exchange contribution," J. Chem. Phys. **141**, 094104 (2014).

[37] F. Neese, F. Wennmohs, A. Hansen, and U. Becker, "Efficient, approximate and parallel hartree-fock and hybrid dft calculations. a 'chain-of-spheres' algorithm for the hartree-fock exchange," Chem. Phys. **356**, 98–1009 (2009).

[38] R. A. Friesner, "Electronic ground state of iron(II)porphyrin. Ab initio SCF and CI calculations and computed electron deformation densities," Chem. Phys. Lett. **116**, 39 (1985).

[39] R. A. Friesner, "Solution of the Hartree–Fock equations by a pseudospectral method: Application to diatomic molecules," J. Chem. Phys. **85**, 1462–1468 (1986).

[40] R. A. Friesner, "Solution of the Hartree–Fock equations for polyatomic molecules by a pseudospectral method," J. Chem. Phys. **86**, 3522 (1987).

[41] J. Olsen and P. Jørgensen, "Solution of the Hartree–Fock equations for polyatomic molecules by a pseudospectral method," J. Chem. Phys. **82**, 3235 (1985).

[42] P. Sałek, O. Vahtras, T. Helgaker, and H. Ågren, "Density-functional theory of linear and nonlinear time-dependent molecular properties," J. Chem. Phys. **117**, 9630 (2002).

[43] J. Kussmann and C. Ochsenfeld, "A density matrix-based method for the linear-scaling calculation of dynamic second- and third-order properties at the Hartree-Fock and Kohn-Sham density functional theory levels," J. Chem. Phys. **127**, 204103 (2007).

[44] A. J. Thorvaldsen, K. Ruud, K. Kristensen, P. Jørgensen, and S. Coriani, "A density matrix-based quasienergy formulation of the kohn–sham density functional response theory using perturbation- and time-dependent basis sets," J. Chem. Phys. **129**, 214108 (2008).

[45] K. Sasagane, F. Aiga, and R. Itoh, "Higher-order response theory based on the quasienergy derivatives: The derivation of the frequency-dependent polarizabilities and hyperpolarizabilities," J. Chem. Phys. **99**, 3738 (1993).

[46] O. Christiansen, C. Hättig, and P. Jørgensen, "Response functions from Fourier component variational perturbation theory applied to a time-averaged quasienergy," Int. J. Quantum Chem. **68**, 1 (1998).

[47] H. Larsen, P. Jørgensen, J. Olsen, and T. Helgaker, "Hartree-Fock and Kohn-Sham atomic-orbital based time-dependent response theory," J. Chem. Phys. **113**, 8908 (2000).

[48] S. Coriani, S. Høst, B. Jansík, L. Thøgersen, J. Olsen, P. Jørgensen, S. Reine, F. Pawłowski, T. Helgaker, and P. Sałek, "A linear scaling implementation of molecular response theory in self-consistent field electronic-structure theory," J. Chem. Phys. **126**, 154108 (2007).

[49] T. Kjærgaard, P. Jørgensen, J. Olsen, S. Coriani, and T. Helgaker, J. Chem. Phys. **129**, 054106 (2008).

[50] D. N. Zubarev, *Nonequilibrium Statistical Mechanics* (Consultants Bureau, New York, 1974).

[51] M. Ringholm, D. Jonsson, and K. Ruud, "A general, recursive, and open-ended response code," J. Comput. Chem. **35**, 622–633 (2014).

[52] D. H. Friese, M. T. P. Beerepoot, M. Ringholm, and K. Ruud, "Open-ended recursive approach for the calculation of multiphoton absorption matrix elements," J. Chem. Theory Comput. **11**, 1129–1144 (2015).

[53] D. H. Friese, M. Ringholm, B. Gao, and K. Ruud, "Open-ended recursive calculation of single residues of response functions for perturbation-dependent basis sets," J. Chem. Theory Comput. **11**, 4814–4824 (2015).

[54] A. H. Steindal, M. T. P. Beerepoot, M. Ringholm, N. H. List, K. Ruud, J. Kongsted, and J. M. H. Olsen, "Open-ended response theory with polarizable embedding: multiphoton absorption in biomolecular systems," Phys. Chem. Chem. Phys. **18**, 28339–28352 (2016).

[55] C. Hättig and F. Weigend, "CC2 excitation energy calculations on large molecules using the resolution of the identity approximation," J. Chem. Phys. **113**, 5154–5161 (2000).

[56] C. Hättig and A. Köhn, "Transition moments and excited-state first-order properties in the coupled-cluster model CC2 using the resolution-of-the-identity approximation," J. Chem. Phys. **117**, 6939–6951 (2002).

[57] C. Hättig and K. Hald, "Implementation of RI-CC2 triplet excitation energies with an application to *trans*-azobenzene," Phys. Chem. Chem. Phys. **4**, 2111–2118 (2002).

[58] C. Hättig, "Geometry optimizations with the coupled-cluster model CC2 using the resolution-of-the-identity approximation," J. Chem. Phys. **118**, 7751–7761 (2003).

[59] A. Köhn and C. Hättig, "Analytic gradients for excited states in the coupled-cluster model CC2 employing the resolution-of-the-identity approximation," J. Chem. Phys. **119**, 5021–5036 (2003).

[60] D. H. Friese, C. Hättig, and K. Ruud, "Calculation of two-photon absorption strengths with the approximate coupled cluster singles and doubles model cc2 using the resolution-of-identity approximation," Phys. Chem. Chem. Phys. **14**, 1175–1184 (2012).

[61] D. H. Friese, N. O. C. Winter, P. Balzerowski, R. Schwan, and C. Hättig, "Large scale polarizability calculations using the approximate coupled cluster model CC2 and MP2 combined with the resolution-of-the-identity approximation," J. Chem. Phys. **136**, 174106 (2012).

[62] D. H. Friese, C. Hättig, and J. Kussmann, "Analytic molecular hessian calculations for cc2 and mp2 combined with the resolution of identity approximation," J. Chem. Theory Comput. **9**, 1469–1480 (2013).

[63] D. H. Friese and C. Hättig, "Optical rotation calculations on large molecules using the approximate coupled cluster model cc2

[63] and the resolution-of-the-identity approximation," Phys. Chem. Chem. Phys. **16**, 5942–5951 (2014).

[64] N. K. Graf, D. H. Friese, N. O. C. Winter, and C. Hättig, "Excited state polarizabilities for CC2 using the resolution-of-the-identity approximation," J. Chem. Phys. **143**, 244108 (2015).

[65] P. Deglmann, K. May, F. Furche, and R. Ahlrichs, "Nuclear second analytical derivative calculations using auxiliary basis set expansions," Chem. Phys. Lett. **384**, 103–107 (2004).

[66] R. Bauernschmitt, M. Häser, O. Treutler, and R. Ahlrichs, "Calculation of excitation energies within time-dependent density functional theory using auxiliary basis set expansions," Chem. Phys. Lett. **264**, 573–578 (1997).

[67] F. Neese and G. Olbrich, "Efficient use of the resolution of the identity approximation in time-dependent density functional calculations with hybrid density functionals," Chemical Physics Letters **362**, 170 – 178 (2002).

[68] S. Grimme, F. Furche, and R. Ahlrichs, "An improved method for density functional calculations of the frequency-dependent optical rotation," Chemical Physics Letters **361**, 321 – 328 (2002).

[69] F. Furche and D. Rappoport, "{III} - density functional methods for excited states: Equilibrium structure and electronic spectra," in *Computational Photochemistry*, Theoretical and Computational Chemistry, Vol. 16, edited by M. Olivucci (Elsevier, 2005) pp. 93 – 128.

[70] D. Rappoport and F. Furche, "Analytical time-dependent density functional derivative methods within the ri-j approximation, an approach to excited states of large molecules," The Journal of Chemical Physics **122**, 064105 (2005), http://dx.doi.org/10.1063/1.1844492.

[71] C. Kumar, T. Kjærgaard, T. Helgaker, and H. Fliegl, "Nuclei-selected atomic-orbital response-theory formulation for the calculation of nmr shielding tensors using density-fitting," The Journal of Chemical Physics **145**, 234108 (2016).

[72] F. London, J. Phys. Radium **8**, 397–409 (1937).

[73] M. Marques and E. Gross, Annual Review of Physical Chemistry **55**, 427–455 (2004).

[74] K. Burke, J. Werschnik, and E. K. U. Gross, The Journal of Chemical Physics **123**, 062206 (2005).

[75] K. Capelle, Brazilian Journal of Physics **36**, 1318 – 1343 (2006).

[76] M. Casida and M. Huix-Rotllant, "Progress in time-dependent density-functional theory," Annual Review of Physical Chemistry **63**, 287–323 (2012).

[77] T. Helgaker, P. Jørgensen, and J. Olsen, *Molecular Electronic–Structure Theory* (Wiley, Chichester, 2000).

[78] T. Helgaker, H. Larsen, J. Olsen, and P. Jørgensen, "Direct optimization of the ao density matrix in hartree-fock and kohn-sham theories," Chem. Phys. Lett. **327**, 397–403 (2000).

[79] H. Larsen, P. Jørgensen, J. Olsen, and T. Helgaker, "Hartree-fock and kohn-sham atomic-orbital based time-dependent response theory," J. Chem. Phys. **113**, 8908–8917 (2000).

[80] L. Boman, H. Koch, and A. Sánchez de Merás, "Method specific Cholesky decomposition: Coulomb and exchange energies," J. Chem. Phys. **129**, 134107 (2008).

[81] R. Izsak and F. Neese, "An overlap fitted chain of spheres exchange method," J. Chem. Phys. **135**, 144105 (2011).

[82] M. Schreiber, M. R. Silva-Junior, S. P. A. Sauer, and W. Thiel, "Benchmarks for electronically excited states: Caspt2, cc2, ccsd, and cc3," The Journal of Chemical Physics **128**, 134110 (2008).

[83] K. Aidas, C. Angeli, K. L. Bak, V. Bakken, R. Bast, L. Boman, O. Christiansen, R. Cimiraglia, S. Coriani, P. Dahle, E. K. Dalskov, U. Ekström, T. Enevoldsen, J. J. Eriksen, P. Ettenhuber, B. Fernández, L. Ferrighi, H. Fliegl, L. Frediani, K. Hald, A. Halkier, C. Hättig, H. Heiberg, T. Helgaker, A. C. Hennum, H. Hettema, E. Hjertenæs, S. Høst, I.-M. Høyvik, M. F. Iozzi, B. Jansík, H. J. Aa. Jensen, D. Jonsson, P. Jørgensen, J. Kauczor, S. Kirpekar, T. Kjærgaard, W. Klopper, S. Knecht, R. Kobayashi, H. Koch, J. Kongsted, A. Krapp, K. Kristensen, A. Ligabue, O. B. Lutnæs, J. I. Melo, K. V. Mikkelsen, R. H. Myhre, C. Neiss, C. B. Nielsen, P. Norman, J. Olsen, J. M. H. Olsen, A. Osted, M. J. Packer, F. Pawlowski, T. B. Pedersen, P. F. Provasi, S. Reine, Z. Rinkevicius, T. A. Ruden, K. Ruud, V. V. Rybkin, P. Sałek, C. C. M. Samson, A. S. de Merás, T. Saue, S. P. A. Sauer, B. Schimmelpfennig, K. Sneskov, A. H. Steindal, K. O. Sylvester-Hvid, P. R. Taylor, A. M. Teale, E. I. Tellgren, D. P. Tew, A. J. Thorvaldsen, L. Thøgersen, O. Vahtras, M. A. Watson, D. J. D. Wilson, M. Ziolkowski, and H. Ågren, "The dalton quantum chemistry program system," Wiley Interdisciplinary Reviews: Computational Molecular Science **4**, 269–284 (2014).

[84] *LSDALTON, a linear scaling molecular electronic structure program, Release Dalton2011* (2011), see http://www.daltonprogram.org/.

[85] T. Yanai, D. P. Tew, and N. C. Handy, "A new hybrid exchange–correlation functional using the coulomb-attenuating method (cam-b3lyp)," Chemical Physics Letters **393**, 51 – 57 (2004).

[86] C. Ochsenfeld, C. A. White, and M. Head-Gordon, "Linear and sublinear scaling formation of hartree–fock-type exchange matrices," J. Chem. Phys. **109**, 1663–1669 (1998).

[87] F. Jensen, "Unifying general and segmented contracted basis sets. segmented polarization consistent basis sets," Journal of Chemical Theory and Computation **10**, 1074–1085 (2014).

[88] F. Weigend, "Hartree–fock exchange fitting basis sets for h to rn †," J. Comput. Chem. **29**, 167–175 (2008).

[89] S. Reine, E. Tellgren, T. Helgaker, U. Ekström, R. Izsak, F. Jensen, and T. Kjærgaard, "Basis sets for the auxiliary-density-matrix method," in preparation (2017).

[90] M. J. G. Peach, P. Benfield, T. Helgaker, and D. J. Tozer, "Excitation energies in density functional theory: An evaluation and a diagnostic test," J. Chem. Phys. **128**, 044118 (2008).

[91] A. J. Cohen, P. Mori-Aánchesz, and W. Yang, "Challenges for density functional theory," Chem. Rev. **112**, 289–320 (2012).

[92] G. Maroulis, "Static hyperpolarizability of the water dimer and the interaction hyperpolarizability of two water molecules," The Journal of Chemical Physics **113**, 1813–1820 (2000), http://dx.doi.org/10.1063/1.481985.

[93] I. M. Kenawia, A. H. Kamelb, and R. H. Hilala, "Bsse effects on the static dipole polarizability and first dipole hyperpolarizability of diclofenac sodium," J. Mol. Struct. (Theochem) **851**, 46–53 (2008), https://doi.org/10.1016/j.theochem.2007.10.034.